Buckling Load and Post-buckling Behavior of Tapered Column with Constant Volume and Both Clamped Ends

일정체적 양단고정 변단면 기둥의 좌굴하중 및 후좌굴 거동

Lee, Byoung Koo* · Oh, Sang Jin**
이 병 구 · 오 상 진
Jin, Tae Ki*** · Lee, Jong Kook***
진 태 기 · 이 종 국

요 약

이 논문은 일정체적을 갖는 양단고정 변단면 기둥의 좌굴하중 및 후좌굴 거동에 관한 연구이다. 기둥의 변단면으로는 직선형, 포물선형, 정현의 선형을 갖는 세 가지 변단면을 채택하였다. Bernoulli-Euler보 이론을 이용하여 압축하중이 작용하여 좌굴된 기둥의 정확탄성곡선을 지배하는 미분방정식을 유도하였다. 유도된 미분방정식을 Runge-Kutta법과 Regula-Falsi법을 이용하여 수치해석하였다. 수치해석의 결과로 좌굴하중, 좌굴기둥의 평형경로 및 정확탄성곡선을 산출하였다. 또한 좌굴하중-단면비 곡선으로부터 최강기둥의 좌굴하중과 단면비를 산출하였다.

I. Introduction

The first study of the elastica was published by Euler.[1] A survey of the classical literature on this subject was published by Schmidt and Da Deppo.[2] Present-day applications of elastica included statics and dynamics problems were discussed by Wilson and Mahajan[3] and Lee *et al.*,[4] respectively. Other works related to the present studies, especially those involving uniform beams, were studied by Love,[5] Timoshenko and Gere,[6] Rojahn,[7] Wang,[8] Wilson and Snyder,[9] Lee[10] and Chucheepsakul *et al.*.[11,12]

Since columns are basic structural forms, these units have been widely used in various engineering fields. In column problems, both the buckling loads and postbuckling behaviors are very important to structural design. The column behavior under loads depends on the cross-sectional shape, taper type and volume of the column.[13] Especially estimating the buckling loads of nonprismatic columns, which have the same volume with specific length,

*원광대학교 공과대학
**담양대학 토목과
***원광대학교 대학원

키워드 : Bernoulli-Euler beam theory, buckling load, constant volume, elastica, equilibrium path, strongest column, tapered column.

are attractive in the viewpoint of optimal design. Since Lagrange[14] attempted to determine the optimum shape for a column, many investigators including Clausen,[15] Keller,[16] Tadjbakhsh and Keller,[17] Barnes,[18] and Cox and Overton[19] determined the shape of the strongest column which is defined as the elastic column of a given length and volume which can carry the highest axial load without buckling. In the most previous works related on the strongest column, only the equilateral triangular, square and circular were considered as the cross-section. Considering the erecting condition and the aesthetic viewpoint, the cross-sections of regular polygon are sometimes needed in the practical engineering fields. Nowhere in the open literature gave the solutions for the class of elastica problems considered herein : the elastica and buckling load of non-uniform or tapered columns of regular polygon cross-section with constant volume, whose cross-sectional depths are varied by functional fashions. Therefore the main purpose of this paper is to investigate both the buckling load and elastica of such columns.

In the analysis of elastica, one usually begins with classical Bernoulli-Euler beam theory and the non-linear differential equation that relates deflection to load. This beam theory is also used in the present analytical studies. The following assumptions are inherent in this theory : the column is linearly elastic, the neutral axis for bending is incompressible, and transverse shear deformations are negligible.

Historically, solutions of elastica have four forms : (1) closed-form solutions in terms of elliptic integrals : (2) power series solutions : (3) numerical solutions : and (4) experimental solutions. The present study should be classified into the numerical solutions.

Ⅱ. Object Column

Shown in Fig. 1(a) is the object column of specific length l and of constant volume V. All the columns analyzed in this study have the same length and the same volume. Its cross-sectional shape is the regular polygon, whose cross-sectional depth depicted as h varies with the axial length s. The area and area moment of inertia of cross section depicted as A and I, respectively, vary with s. Fig. 1(b) shows the variation of depth h with s. As shown in this figure, the depth h is varied by functional fashion, and depths h at $s=0$ and l, and at $s=l/2$ are h_0 and h_m, respectively. For defining geometry of column, a non-dimensional system parameter or section ratio n is introduced as follows.

$$n = h_m/h_0 \cdots\cdots (1)$$

The area A and area moment of inertia of cross section I of the regular polygon cross-section with integer m of side number

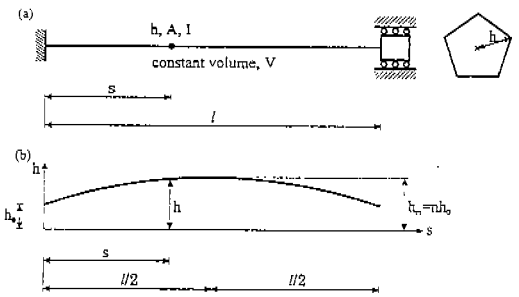

Fig. 1. Column with constant volume and its variation of cross-sectional depth

and cross-sectional depth h are given by equations (2) and (3), respectively.

$$A = c_1 h^2 \quad \cdots\cdots(2)$$

$$I = c_2 h^4 \quad \cdots\cdots(3)$$

where

$$c_1 = m \sin(\pi/m)\cos(\pi/m) \quad \cdots\cdots(4.1)$$

$$c_2 = m \sin(\pi/m)\cos^3(\pi/m)[1+\tan^2(\pi/m)/3]/4 \quad \cdots\cdots(4.2)$$

in which it is clear that values of c_1 and c_2 with infinite number $m(\infty)$, namely circular cross-section, are converged to π and $\pi/4$, respectively. Also, it is noted that every axis across the centroid of regular polygon cross-section is a principal axis and has the same area moment of inertia of cross section given in equation (3).

Now, consider the functional equations of variable depth h. It is natural that all columns whose variable depth are prescribed should be the object ones. In this study, the linear, parabolic and sinusoidal tapers are chosen as the variable depth h of tapered columns. First, the equations h of linear taper through three points of (0, h_0), ($l/2$, nh_0) and (l, h_0) in rectangular co-ordinates (s, h) are obtained as follows.

$$\left.\begin{aligned} h &= h_0[2c_3(s/l)+1], \quad 0 \le s \le l/2 \\ h &= h_0[-2c_3(s/l)+2c_3+1], \quad l/2 \le s \le l \end{aligned}\right\} \quad \cdots(5)$$

where

$$c_3 = n-1 \quad \cdots\cdots(6)$$

The column's volume V can now be calculated by using equations (2) and (5) :

$$V = \int_0^l A ds = c_4(c_1 h_0^2 l) \quad \cdots\cdots(7)$$

where

$$c_4 = V/(c_1 h_0^2 l) = (n^2+n+1)/3 \quad \cdots\cdots(8)$$

In the above equation, c_4 is defined as a ratio of constant volume V to volume of uniform column of regular polygon cross-section with depth h_0, $c_1 h_0^2 l$.

Second, the equations h and c_4 of parabolic taper are given by equations (9) and (10), respectively.

$$h = h_0[-4c_3(s/l)^2+4c_3(s/l)+1], \quad 0 \le s \le l \quad \cdots\cdots(9)$$

$$c_4 = (8n^2+4n+3)/15 \quad \cdots\cdots(10)$$

Finally, the equations h and c_4 of sinusoidal taper are as follows, respectively.

$$h = h_0[c_3 \sin(\pi s/l)+1], \quad 0 \le s \le l \quad \cdots\cdots(11)$$

$$c_4 = (n-1)^2/2 + 4(n-1)/\pi + 1 \quad \cdots\cdots(12)$$

In equations (9) and (11), c_3 is defined in equation (6).

Ⅲ. Mathematical Model

The symbols and loading for the column defined in above section are depicted in Fig. 2. The clamped-clamped ends support the column. The column subjected to a compressive end load P less than the buckling load B is perfectly straight. But when the P exc-

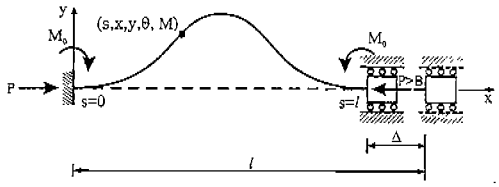

Fig. 2. Variables of elastica of buckled column

eeds the B, the column is buckled. The dashed line and the solid curve are the neutral axes of the unbuckled and buckled column, respectively. Thus the shape of elastica is the solid curve defined by the (x, y) co-ordinate system whose origin is at left end. At material point (x, y), the column's arc length is s, and the variable area and area moment of inertia of cross section taken with respect to s are A and I, respectively. The rotation of cross-section and bending moment are depicted as θ and M, respectively, in this figure. It is noted that the axis length of buckled column maintains its length l due to incompressibility of column, and therefore the s value at right end is l. The end moments at both ends ($s=0$ and $s=l$) and the horizontal displacement at right end ($s=l$) are M_0 and Δ, respectively. It is assumed that Bernoulli-Euler theory governs the buckled column behavior under load, for which the differential equations for the elastica are as follows.[6]

$$d\theta/ds=(M_0-Py)/EI,\quad 0\le s\le l \cdots\cdots(13)$$

$$dx/ds=\cos\theta,\quad 0\le s\le l \cdots\cdots(14)$$

$$dy/ds=\sin\theta,\quad 0\le s\le l \cdots\cdots(15)$$

where E is Young's modulus and the term of (M_0-P_y) in equation (13) is the bending moment M at the material point (x, y).

Since the horizontal and vertical displacements, and rotation at left end ($s=0$) are not allowed, the following boundary conditions are obtained :

$$x=0 \text{ at } s=0 \cdots\cdots(16)$$

$$y=0 \text{ at } s=0 \cdots\cdots(17)$$

$$\theta=0 \text{ at } s=0 \cdots\cdots(18)$$

Since the rotation at mid-point of column axis ($s=l/2$) is zero due to the symmetry of column geometry, the boundary condition is given by equation (19).

$$\theta=0 \text{ at } s=l/2 \cdots\cdots(19)$$

To facilitate the numerical studies and to obtain the most general results for this class of problem, the axial load, the end moment, the geometric parameters, and the governing differential equations with their boundary conditions are cast in the following non-dimensional forms.

The load parameters p and m_0 are defined as equations (20) and (21).[20]

$$p=P l^2/(\pi^2 EI_c) \cdots\cdots(20)$$

$$m_0=M_0 l/(\pi^2 EI_e) \cdots\cdots(21)$$

where I_e is the area moment of inertia of circular cross-section of uniform column whose volume is V, defined as equation (22).

$$I_e=V^2/(4\pi l^2) \cdots\cdots(22)$$

It is noted that the load parameters p and m_0 are defined by using the constant volume

V and the specific length l in order to compare all the responses of columns regardless of taper type, side number m and section ratio n.

The arc length s and coordinates (x, y) are normalized by the column length l.

$$\lambda = s/l \quad \cdots\cdots(23)$$

$$\xi = x/l \quad \cdots\cdots(24)$$

$$\eta = y/l \quad \cdots\cdots(25)$$

The displacement Δ of right end ($s = l$) is also normalized by l.

$$\delta = \Delta/l \quad \cdots\cdots(26)$$

When equation (3) is combined with either equation (5) or equation (9) or equation (11), and equations (20)~(25) are used, the non-dimensional form of equation (13) becomes as follows.

$$d\theta/d\lambda = \pi c_1^2 c_4^2 (m_0 - p\eta)/(4c_2 i),\ 0 \le \lambda \le 1 \quad \cdots(27.1)$$

where

for linear taper :

$$\left.\begin{aligned} i &= (2c_3\lambda + 1)^4,\ 0 \le \lambda \le 0.5 \\ i &= (-2c_3\lambda + 2c_3 + 1)^4,\ 0.5 \le \lambda \le 1 \end{aligned}\right\} \quad \cdots\cdots(27.2)$$

for parabolic taper :

$$i = (-4c_3\lambda^2 + 4c_3\lambda + 1)^4,\ 0 \le \lambda \le 1 \quad \cdots\cdots(27.3)$$

for sinusoidal taper :

$$i = [c_3 \sin(\pi\lambda) + 1]^4,\ 0 \le \lambda \le 1 \quad \cdots\cdots(27.4)$$

It is recalled that the coefficients c_1-c_4 of differential equation (27.1) with equations (27.2)~(27.4) contain the side number m and section ratio n, respectively, as shown in the previous section.

Further, with equations (23)~(25), equations (14) and (15) become as follows.

$$d\xi/d\lambda = \cos\theta,\ 0 \le \lambda \le 1 \quad \cdots\cdots(28)$$

$$d\eta/d\lambda = \sin\theta,\ 0 \le \lambda \le 1 \quad \cdots\cdots(29)$$

The non-dimensional forms for boundary conditions of equations (16)~(19) are obtained by equations (23)~(25):

$$\xi = 0 \text{ at } \lambda = 0 \quad \cdots\cdots(30)$$

$$\eta = 0 \text{ at } \lambda = 0 \quad \cdots\cdots(31)$$

$$\theta = 0 \text{ at } \lambda = 0 \quad \cdots\cdots(32)$$

$$\theta = 0 \text{ at } \lambda = 1/2 \quad \cdots\cdots(33)$$

Ⅳ. Numerical Methods

Based on above analysis, the algorithm was developed to solve differential equations (27.1), (28) and (29). The Runge-Kutta and Regula-Falsi methods[21] were used to integrate differential equations and to determine the end moment m_0 at $\lambda = 0$ for a given geometry of column. This algorithm is summarized as follows.

(1) Specify taper type (linear/parabolic/sinusoidal), geometry (m and n), and load p. Calculate c_1-c_4. It is recalled that m is the integer number of sides of regular polygon cross-section.

(2) Assume a trial value $m_{0(t)}$ in which first trial value is zero.

(3) Integrate equations (27.1), (28) and

(29) with the boundary conditions of equations (30)~(32) in the range from $\lambda=0$ to 1/2 using the Runge-Kutta method. The results give trial solutions for $\theta=\theta(\lambda)$, $\xi=\xi(\lambda)$ and $\eta=\eta(\lambda)$.

(4) Set $D=\theta(1/2)$. If the value of $m_{0(t)}$ assumed in step 2 is the characteristic value of the elastica, then D must be zero due to equation (33). The first criterion for convergence of the solutions is $|D| \leq 1\times10^{-10}$.

(5) If the value of D does not satisfy the first convergence criterion, then increment the previous value of $m_{0(t)}$.

(6) Repeat steps (3)~(5) and note the sign of D in each iteration. If D changes sign between two consecutive values $m_{0(1)}$ and $m_{0(2)}$ of $m_{0(t)}$, then the characteristic value m_0 lies between $m_{0(1)}$ and $m_{0(2)}$.

(7) Compute an improved value of $m_{0(t)}$ based on its two previous values using the Regula-Falsi method. The second criterion for convergence of solutions is $|(m_{0(2)}-m_{0(1)})/m_{0(2)}| \leq 1\times10^{-5}$.

(8) Terminate the calculations when two convergence criteria are met. Print the final solutions to the elastica, $\theta=\theta(\lambda)$, $\xi=\xi(\lambda)$ and $\eta=\eta(\lambda)$, and then compute the displacement $\delta=1-2\xi(1/2)$. It is noted that θ, ξ and η in the range of $1/2<\alpha\leq1$ can be calculated by the symmetry of column geometry. If there is no solution, which means that D does not change sign till the trial value of $m_{0(t)}$ reaches p/2 because the m_0 value can not be larger than p/2 physically, the specified p is less than b and the column is still straight. Here, b is the buckling load parameter defined as follows.[20]

$$b=B\ell^2/(\pi^2EI_e) \quad \cdots\cdots(34)$$

Also, the buckling load parameters b were calculated in a straightforward way using the differential equations. Just after the column is buckled, all values of column behavior including m_0 are close to zero. In this study, the buckling load parameter b is approximately equivalent to the load parameter p whose end moment m_0 is 1×10^{-10}, i.e. nearly zero but not zero. Specify column taper, m, n, of course not p and set $m_0=1\times10^{-10}$ in equation (27.1). And assume the trial value p instead of $m_{0(t)}$ in step 2. Remaining numerical procedures are same as above procedure, and of course the characteristic value of equation (27.1) is p which is now an approximate buckling load parameter b.

Based on these algorithms, two FORTRAN computer programs were written to solve the elastica and buckling load, respectively. All computations were carried on a notebook computer with graphics support. For all of the numerical results presented herein, a step size of $\Delta\lambda=(1/2)/50$ in the Runge-Kutta method was found to give convergence for m_0 and b to within three significant figures. The numerical results are now discussed in next section.

V. Numerical Results and Discussions

First considers the elastica problem. Shown in Fig. 3 are the equilibrium paths of linear taper with m=3, 4 and c (circular cross-section) for n=0.5, which represent the end moment m_0 and deflections (δ and η_m) versus p curves after buckling. Here, η_m is defined as value of η at column's mid-point ($\lambda=1/2$). The nonlinear responses of m_0 and δ increase as p increases; those of η_m reach

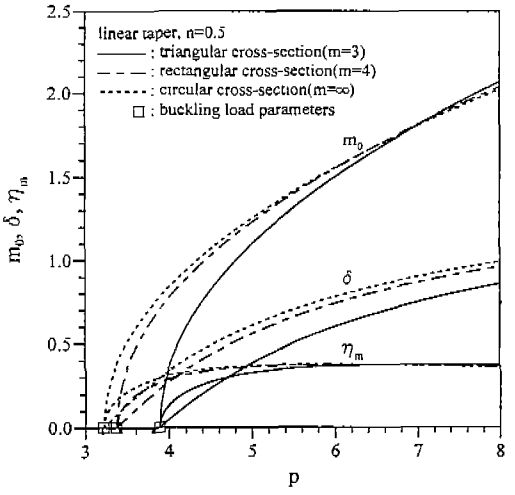

Fig. 3. Equilibrium path of linear taper with n=0.5 by side number m

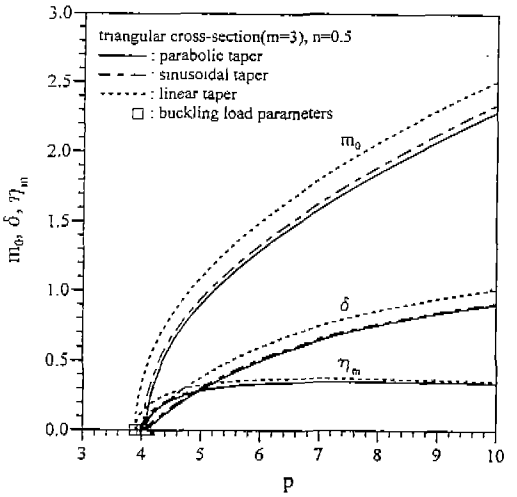

Fig. 4. Equilibrium path of columns with m=3 and n=0.5 by taper type

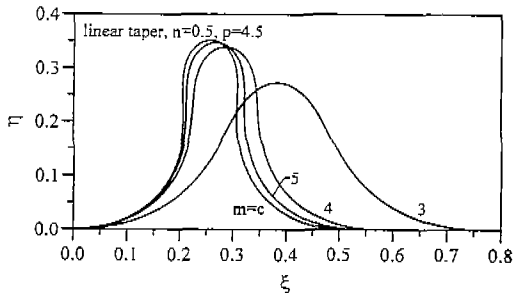

Fig. 5. Elastica of linear taper with n=0.5 and p=4.5 by side number m

peaks as p is increased. The increasing rates of all responses are higher in lower p. Especially the rates are very high just after the columns are buckled. Just after buckling of the column, as the integer number m increases from m=3 to m=4 to m=c (∞), all responses increase, other parameters remaining constant. But it is true that in case of response m_0 and η_m, the fact is reversed when p exceeds some characteristic value. It is seen that the p values marked by □ are the buckling load parameters b of corresponding columns. For example, the b of m=3 is 3.888.

Shown in Fig. 4 are the equilibrium paths of parabolic, sinusoidal and linear tapers for m=3 and n=0.5. Just after buckling, as the taper type is changed from parabolic to sinusoidal to linear taper, the response of m_0 increases corresponding to this change, other parameters remaining constant. Also, the buckling load parameters are marked by □ on the p axis.

Figure 5 shows the elastica of linear taper with m=3, 4, 5 and c for n=0.5 and p=4.5. From this figure, as the m value increases from 3 to c, the horizontal and vertical deflections increase.

Second considers the buckling load problem. For the purpose of validation of this study, the buckling load parameters b predicted by the present theory are compared to those available in references in Table 1 which shows the results of this study agree quite well with the reference values.

Shown in Figs. 6-8 are the b versus n

Table 1. Comparisons of b between this study and references

Geometry	Buckling load parameter, b		
	This study	Reference	
n=1.*, m=c	b=4.0	4.0 of ref.[A]+	
n=0.836, m=3	b=4.929	4.927	of ref.[A]+
n=0.836, m=4	b=4.269	4.270	
n=0.836, m=5	b=4.145	4.145	
n=0.836, m=c parabolic	b=4.076	4.076	

*If n=1., the columns are uniform regardless of taper types. See equations (27.2)~(27.4)
+[A] : Timoshenko and Gere[6], [B] : Lee and Oh[20]

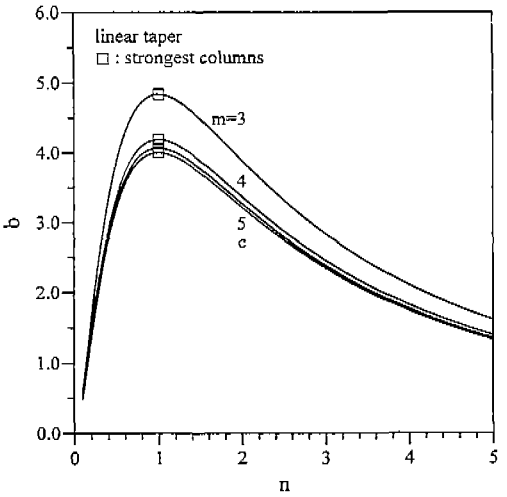

Fig. 6. b vs. n curves of linear taper by side number m

curves of columns with m=3, 4, 5 and c for linear, parabolic and sinusoidal taper, respectively. Each curve reaches a peak which is marked by □. At these peak points, the columns corresponding to the given taper types show the largest b values, which are the buckling load parameters of strongest columns. Here the word "strongest" is used to mean "most" resistant to buckle. It is found that all strongest columns occur at the same value n regardless of side number m if the taper type is same. And all b values of

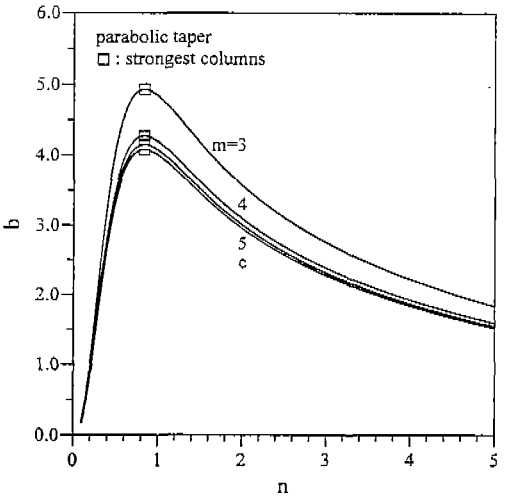

Fig. 7. b vs. n curves of parabolic taper by side number m

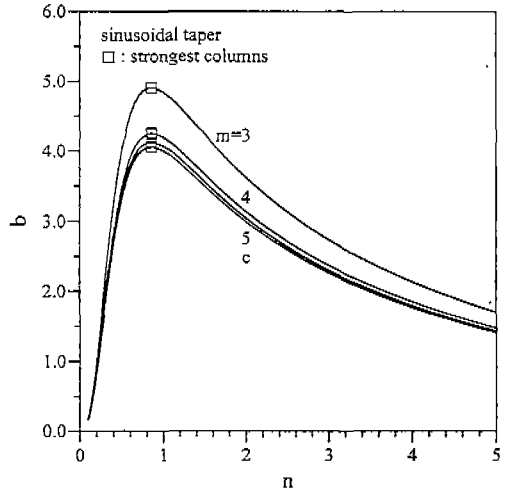

Fig. 8. b vs. n curves of sinusoidal taper by side number m

strongest columns decrease, as the m value is increased from 3 to c. The values of b and n of all strongest columns are summarized in Table 2. From this table, it is noted that all b values of strongest columns are largest at m=3(triangular cross-section) and smallest at m=c(circular cross-section), and the ratios of m=3 to m=c are same, i.e. 1.210, regardless

Table 2. Values of n and b of strongest columns by taper type and side number m

Taper type	m	n	b	ratio*
Linear taper	3	1.00	4.837	1.210
	4	1.00	4.189	1.047
	5	1.00	4.068	1.017
	c	1.00	4.000	1.000
Parabolic taper	3	0.836	4.929	1.210
	4	0.836	4.269	1.047
	5	0.836	4.145	1.017
	c	0.836	4.075	1.000
Sinusoidal taper	3	0.855	4.904	1.210
	4	0.855	4.247	1.047
	5	0.855	4.124	1.017
	c	0.855	4.056	1.000

*Ratio of b of m=3, 4 and 5, respectively, to m=c

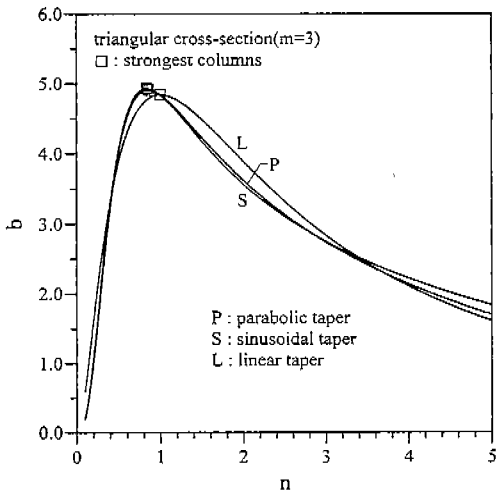

Fig. 9. b vs. n curves by taper type

of taper types.

Shown in Fig. 9 are the b versus n curves of parabolic, sinusoidal and linear tapers, respectively, for m=3, in which the strongest columns are marked by □. It is clear that the strongest of all columns by taper type is the parabolic tapered column as shown in this figure and Table 2. The effect of taper type on b is negligible when n is less than about 0.4.

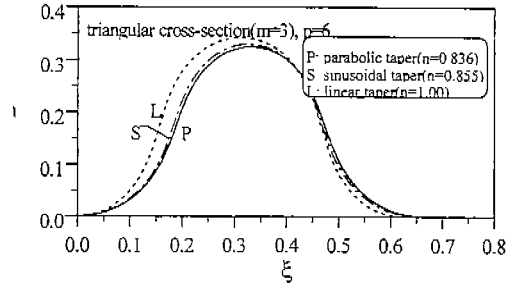

Fig. 10. Elastica of strongest columns with m=3 and p=6

Shown in Fig. 10 are the elastica of strongest columns of m=3 and p=6 by taper type. It is clear that the horizontal and vertical deflections increase, as the taper type is increased from parabolic to sinusoidal to linear taper, other parameters remaining constant.

VI. Concluding Remarks

The numerical methods developed herein for computing the elastica and buckling load of tapered column of regular polygon cross-section with constant volume and both clamped ends were found to be efficient, and highly versatile. The differential equations governing the elastica of such column were derived and solved numerically. The linear, parabolic and sinusoidal tapers were chosen for the variable cross-sectional depth. As the numerical results, the equilibrium paths and elastica were presented, and the buckling load parameters versus section ratio (b vs. n) curves were also reported. The strongest columns by taper type and side number of regular polygon cross-section were determined by reading the peak point of buckling load parameters and their corresponding section ratios on b versus n curves. The effect of taper type on buckling load parameters is negligible

when section ratio is less than about 0.4.

Acknowledgement

This paper was supported by Wonkwang University in 1999. The first author thanks for this financial support.

References

1. Euler, L., 1774, "Methodus Inveniendi Lineas Curvas Maxima Minimive Proprietate Gaudentes," Additamentum I. De Curvis Elasticis. Lausanne and Geneva.
2. Schmidt, R. and Da Deppo, D. A., 1971, "A survey of literature on large deflection of nonshallow arches, bibliography of finite deflections of straight and curved beams, rings, and shallow arches," The Journal of the Industrial Mathematics Society, Vol. 21, pp. 91-114.
3. Wilson, J. F. and Mahajan, U., 1989, "The mechanics and positioning of highly flexible manipulator limbs," Journal of Mechanism, Transmissions, and Automation Design Vol. III, pp.232-235.
4. Lee, B. K., Wilson, J. F. and Oh, S. J., 1993, "Elastica of cantilevered beams with variable cross-section," International Journal of Non-Linear Mechanics, Vol. 28, pp. 579- 589.
5. Love, A. E. H., 1927, A Treatise on the Mathematical Theory of Elasticity. Dover.
6. Timoshenko, S. P. and Gere, J. M., 1961, Theory of Elastic Stability. McGraw-Hill.
7. Rojahn, C., 1968, Large deflections of elastic beam. Thesis for the Degree of Engineer, Stanford University.
8. Wang, C. Y., 1981, "Large deflections of an inclined cantilever with an end load," International Journal of Non-Linear Mechanics, Vol. 16, pp. 155-164.
9. Wilson, J. F. and Snyder, J. M., 1988, "The elastica with end-load flip-over," Journal of Applied Mechanics, ASME, Vol. 55, pp. 845-848.
10. Lee, B. K., 1990, "Numerical analysis of large deflections of cantilever beams," Journal of Korean Society of Civil Engineers, Vol. 10, pp. 1-7.
11. Chucheepsakul, S., Buncharon, S. and Huang, T., 1995, "Elastica of simple variable-arc-length beams subjected to end moment," Journal of Engineering Mechanics, ASCE, Vol. 121, pp. 767-772.
12. Chucheepsakul, S., Thepphitak, G. and Wang, C. M., 1996, "Large deflection of simple variable-arc-length beams subjected to a point load," Structural Engineering and Mechanics, Vol. 4, pp. 49-59.
13. Gere, J. M. and Timoshenko, S. P., 1984, Mechanics of Materials. Brooks/Cole Engineering Division.
14. Lagrange, J. L., 1770-1773, "Sur la Figure des Colonnes," Miscellanea Taurinensia. Vol. 5, p. 123. Summarized in Todhunter, I. and Pearson, K., 1886, A History of the Theory of Elasticity and of the Strength of Materials. Cambridge Press.
15. Clausen, T., 1849-1853, "Uber lie Form architektonischer Saulen," Bulletin Physico-Mathematiques et Astronumiques, pp. 279-294. Summarized in Todhunter, I. and Pearson, K., 1893, A History of the Theory of Elasticity and of the Strength of Materials, Cambridge Press.
16. Keller, J. B., 1960, "The shape of the strongest column," Archive for Rational Mec-

hanics and Analysis, Vol. 5, pp. 275-285.
17. Tadjbakhsh, I. and Keller, J. B., 1962, "Strongest columns and isoperimetric inequalities for eigenvalues," Journal of Applied mechanics, ASME, Vol. 29, pp. 159-164.
18. Barnes, D. C., 1988, "The shape of the strongest column is arbitrarily close to the shape of the weakest column," Quarterly of Applied Mathematics, Vol. 46, pp. 605-609.
19. Cox, S. J. and Overton, M. I., 1992, "On the optimal design of columns against Buckling," SIAM Journal on Mathematical Analysis, Vol. 23, pp. 287-325.
20. Lee, B. K. and Oh, S. J., "Free vibrations and buckling loads of tapered columns of regular polygon cross-section with constant volume," International Journal for Numerical Methods in Engineering (in review at present time).
21. Carnahan, B., Luther, H. A. and Wilkes, J. O., 1969, Applied Numerical Methods, John Wiley & Sons.